Magnetic fine structure of domain walls in iron films observed with a magnetic force microscope

Roger Proksch, Sheryl Foss, E. Dan Dahlberg, and Gary Prinz

Citation: Journal of Applied Physics **75**, 5776 (1994); doi: 10.1063/1.355613
View online: http://dx.doi.org/10.1063/1.355613
View Table of Contents: http://scitation.aip.org/content/aip/journal/jap/75/10?ver=pdfcov
Published by the AIP Publishing

Magnetic fine structure of domain walls in iron films observed with a magnetic force microscope

Roger Proksch,[a] Sheryl Foss, and E. Dan Dahlberg
School of Physics and Astronomy, University of Minnesota, Minneapolis, Minnesota 55455

Gary Prinz
Naval Research Laboratory, Washington, D.C. 20375

The submicron magnetic structure of domain walls in a single-crystal iron film has been studied using a magnetic force microscope (MFM). The MFM tip was sensitized to the component of the field perpendicular to the film plane. The sample examined was a 500-nm-thick single-crystal film of iron, grown by molecular-beam epitaxy (MBE). Before it was imaged, the film was magnetized along its (in-plane) easy axis in a 2000-Oe field. Studies of the domain structure at numerous locations on the film surface revealed a rich variety of micromagnetic phenomena. Parallel domain walls, determined to be Bloch walls with a width of 70–100 nm, were seen along the easy axis, spaced roughly 30 μm apart. These appeared to be Bloch walls. Bloch lines were also observed in the walls with an average periodicity of 1.5 μm. This is a value smaller than that predicted for Bloch wall-line structures. In addition, a pronounced zig–zag structure was observed, as expected from previous Fe whisker observations.

The sample examined in this work was an epitaxially grown single crystal of iron, grown in the (110) plane.[1] It is a bcc, α-Fe crystal with unit cell $a=2.866$ Å, grown on a fcc (110) GaAs substrate. The single-crystal nature of the film has been verified by x-ray analysis and magnetic measurements. In the images presented here, the vertical axis corresponds to the [001] axis of the film. The hard axes are the [111] body diagonals, 55° away from the [001], and the intermediate [110] axis is oriented 90° from the [100].

Representative high-resolution images of the (110) surface of a 0.5-μm-thick, epitaxially grown iron film are shown in Figs. 1 and 2. The images were acquired using a Nanoscope III scanning probe microscope from Digital Instruments. The microscope was operated in the tapping/lift™ mode. This technique allows the separation of the topography from the long-range, magnetic forces. A good example of this is shown in Fig. 1 where the magnetic signal from a domain wall is shown on the left and the associated surface topography is shown on the right. For this work, the noncontact scan height was maintained at 50 nm.

The MFM probes used in this study were microfabricated Si cantilevers coated with 30 nm of a CoCr alloy. This coating was optimized for best response and resolution of the MFM. When imaging with an MFM, one concern is that stray fields from the magnetic tip can modify the micromagnetic structure of the sample.[2] An experimental test for this can be made by observing the dependence of the micromagnetic structure on the MFM tip scan height.[3] For the iron samples studied in this work, there was no variation of the sample micromagnetic structure when the tip scan height was varied between 20 and 250 nm. Accordingly, for the remainder of this work, we will assume that modification of the micromagnetic sample structure by the tip is negligible.

The importance of being able to separate topography and magnetism is especially apparent when examining the 15-μm-square scan above part of the iron film shown in Fig. 1. In this figure, the vertical axis corresponds to the [001] magnetic easy axis of the film, and the horizontal axis to the [110] intermediate axis. The [111] hard axis is oriented 55° away from the vertical [001] axis.

Because the MFM is sensitive to the stray field gradients and not the magnetization itself, it is not possible to determine the magnetization in regions where it is constant (e.g., in the middle of a domain). In the case of this sample, however, we are "fortunate" enough to have a number of scratches in the film surface. Where the magnetization intersects these imperfections, magnetostatic charge builds up, resulting in stray magnetic fields that can be detected with the MFM. By observing the polarity of the stray fields from a scratch, it is possible to get an idea of the projection of the magnetization onto the line of the scratch. Thus, the presence of normally unwanted flaws in the sample allow statements about the magnetization that would otherwise be impossible to make.

Using this, we can return to Fig. 1 and immediately observe several "scratch signatures" in the magnetic image. These can be used to verify the presence of a domain wall and assign directions to the magnetization of the two identifiable domains in the image. Specifically, there is a deep scratch running horizontally along the upper quarter of the topographical image of Fig. 1. An examination of the corresponding section of the magnetic image shows stray fields above the scratch. On the left of the bright vertical line in the magnetic image, the contrast is bright (attractive interaction) on the top and dark (repulsive interaction) on the bottom. When the scratch crosses the vertical line, this flips to dark

[a]Present address: Dept. of Physics, St. Olaf College, Northfield, MN.

 0021-8979/94/75(10)/5776/3/$6.00

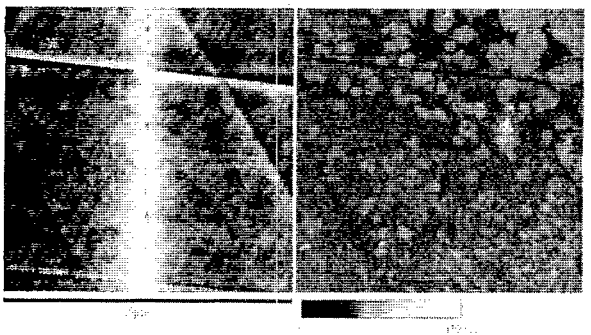

FIG. 1. A 15-μm-square scan of a domain wall. The left image is the magnetic signal and the right is the associated topographical image. In the magnetic image, the direction of the magnetization is clearly visible from the stray fields above the scratches running horizontally through the image. On the left-hand side of the domain wall, the stray fields above the scratches are attractive (bright) on the top and repulsive (dark) on the bottom. The situation is reversed on the right-hand side of the domain wall. Also clearly visible is a wide, bright envelope superimposed on the narrow Bloch line structure. The scale bar is for the topographical image on the right.

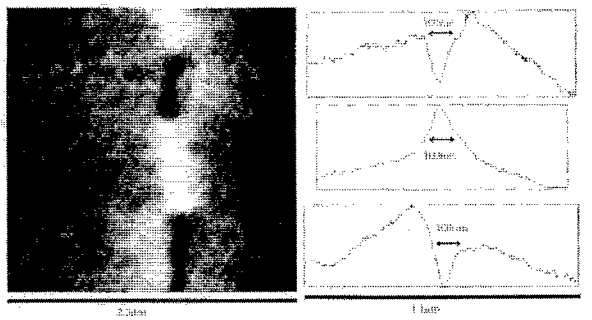

FIG. 2. The gray scale image on the left is a 2.5-μm zoom onto a section of the domain wall of Fig. 1. The three traces on the right-hand side of the figure are average wall profiles obtained by averaging roughly 50 line scans made across each of the two dark and center bright wall segments in the gray scale image.

on the top and bright on the bottom. Thus, we can infer that the [100] component of the magnetization flips across the vertical line, i.e., the vertical line is a domain wall. This effect is visible to a lesser extent in a horizontal scratch near the bottom of the figure.

The Bloch wall seen in Fig. 1 contains many remarkable features. Figure 2 is a 2.5-μm-square high-resolution image of a section of the domain wall in Fig. 1. Also shown in Fig. 2 are three traces which are averaged wall profiles for the two dark and middle bright wall segments shown in the magnetic image. There are a number of observations that can be made of both of these figures. These include:

(i) Alternating dark and bright segments indicative of Bloch lines in the domain wall. Alternating wall segments are visible in all the images.

(ii) Zig–zag structure, where the joints of the zig–zag are the points where the dark and bright segments connect. This zig–zag effect is visible in every image.

A qualitative explanation of features (i) and (ii) follows from simple magnetostatic energy considerations and was provided by Shtrikman and Treves.[4] When a Bloch wall encounters a surface, there is a buildup of magnetostatic charge on the surface. By alternating the sense of the wall rotation, the sign of the charge on the surface also alternates, reducing the magnetostatic energy. The loss of magnetostatic energy is offset by a gain in wall energy associated with the transition regions between the wall segments with opposite rotation senses. Through a simple energy approximation method, Shtrikman and Treves predicted the relationship between the period of the segmented wall T and the thickness of the film L to be $T/L \sim 0.38$ for iron. For the sample studied here we observed an average of $T/L = 1.1$, significantly larger than the predicted. Shtrikman and Treves also explained that the magnetostatic energy could be further reduced if the Bloch wall becomes canted along the line of the wall, resulting in a surface zig–zag structure.

(iii) The sharp, Bloch wall-like section of the wall is always 70–100 nm wide.

(iv) Diffuse, overall bright (or dark) signal superimposed on the wall that is at least three to four times as wide as the alternating segments of the wall. This sort of structure is visible in all the images.

These observations [(iii) and (iv)] can be compared to a number of predictive calculations. First, both Hubert[5] and Scheinfein *et al.*[6] have predicted a Néel-type structure near the surface which caps the bulk Bloch wall. The film modeled in Scheinfein and co-workers was a 0.5-μm-thick single crystal of iron. Their work makes testable predictions and leads to a qualitative understanding of at least some of the features observed here. Their calculations predict that within the bulk of the sample, the transition takes the form of a Bloch wall. The width of the calculated wall in the bulk was within 5% of the classical uniaxial result of $\delta = \kappa(A/K)^{1/2}$. For a magnetic crystal with uniaxial anisotropy, $\kappa = \pi$, and the calculation gives $\delta = 70$ nm. At the surface, the Bloch walls curl in response to demagnetizing fields to form Néel walls. In this calculation the Néel "cap" of the wall is at least 300-nm wide, more than three times the bulk Bloch wall value. According to Lilley,[7] cubic anisotropy has the effect of changing the prefactor κ. Following Lilley, for a domain wall where the direction of the normal to the boundary is along the [110] axis, the prefactor becomes $\kappa = 5.6$. Thus, by including the cubic nature of the anisotropy, the domain wall width is predicted to be $\delta = 125$ nm. This is a value roughly 25–50 nm larger than that observed. Hartmann[8] extended some of these calculations to include surface demagnetizing effects. For iron at room temperature, Hartmann calculated $\kappa = 9.03$ for a domain wall well below the surface. At the surface, the wall narrows considerably to $\kappa = 0.7$. Translated into distances, this implies the bulk wall is $\delta^{(\text{bulk})} = 200$ nm and the surface wall is $\delta^{(\text{surface})} = 15$ nm. This calculation is based on the spatial extent of the vertical component of the magnetization and does not preclude the Néel cap effect predicted by Hubert and Scheinfein *et al.* Given the large range of predictions, the measured wall widths are reasonable. A final note concerning the wall widths is that the CoCr film on the cantilever was on the order of 50 nm, so we would expect the magnetic resolution of the cantilever to be on that scale or larger.

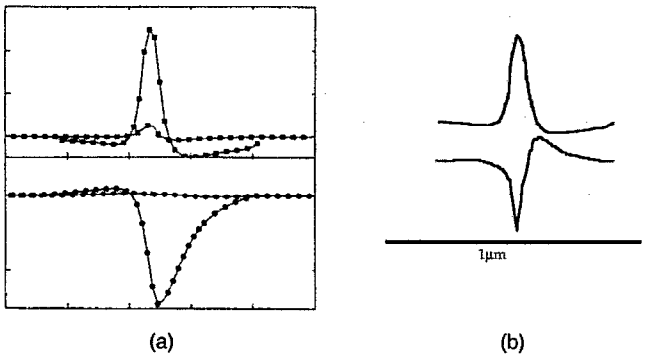

FIG. 3. (a) The results of the micromagnetic calculation of Scheinfein *et al.* for a 0.5-μm-thick iron film. The magnetization as a function of position in a domain wall is shown at the surface of the film (denoted "surface") and in the middle of the film (denoted "bulk"). At the top, the vertical component of the magnetization in both regions is plotted and the bottom two curves show the component perpendicular to the wall plane. (b) The magnetostatic charge densities obtained from the magnetization curves in (a).

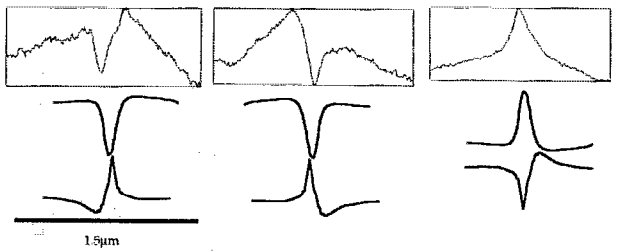

FIG. 4. From symmetry arguments, the wall structure resulting from the model of Scheinfein *et al.* can take on four possible permutations. Three of them were chosen as "best fits" for the averaged wall profiles shown in Fig. 2. Although there is rough qualitative agreement between the experimental averages and a combination of the charge distributions, there are some important disparities. The most obvious is the long wavelength signal in the experimental data that is not present in the charge distributions.

The MFM is sensitive to stray fields arising from magnetostatic charge from the divergence of the magnetization ($\rho_M = -\nabla \cdot \mathbf{M}$). In the following analysis, we will hypothesize that the MFM responds to a combination of magnetostatic charges at and below the sample surface. To qualitatively calculate the magnetostatic charge, we will use the two-dimensional wall calculation of Scheinfein *et al.* The magnetization as a function of position resulting from this model is plotted in Fig. 3(a). For this model, there are two divergence terms that contribute to the charge, $\rho_x = -\partial M_x/\partial x$ and $\rho_z = -\partial M_z/\partial z$. Referring to Fig. 3(a), we can see that at the surface there is only a very small vertical component of the magnetization. Thus, between the middle of the crystal (we will refer to this as the "bulk") and the surface there is a significant amount of magnetostatic charge originating from the divergence of the z component of the magnetization. Although a quantitative statement about the magnitude of this charge cannot be made from observations of the differences between the M_z surface and bulk curves in Fig. 3(a), we can see that the distribution of ρ_z is symmetric about the center of the wall and is roughly 150-nm wide. Thus, for qualitative purposes, we will assume it has the form of the M_z curve [see Fig. 3(b)]. If we extend this result to three dimensions, this should be the charge responsible for the Bloch lines observed in the MFM images.

Returning to the surface [Fig. 3(a)], we also see that the x component of the magnetization has significant divergence. The charge density from the x divergence of the magnetization ρ_x, where $\rho_x = -\partial M_x/\partial x$ at the surface is plotted qualitatively in Fig. 3(b). It is this contribution to the charge which may lead to the wide, diffuse signal surrounding the narrow Bloch line structure of the walls. The total magnetostatic charge which results in the stray fields measured by an MFM should be the sum of these two curves. Plots of the charge density from the bulk ρ_z and the surface ρ_x and the three traces from Fig. 2 are plotted in Fig. 4.

A qualitative comparison of the calculated charge densities to the observed wall profiles (Fig. 4) shows a number of disparities. In particular, although the width of the narrow portion of the domain walls agrees with the models, there is an overall curve superposed on each of the walls which, if originating from ρ_x, is much larger than expected. This is the bright, diffuse structure observed in almost all of the magnetic images. An explanation for this large scale structure is still needed from micromagnetic models. In addition, the length scales of the asymmetries observed in the experimental traces do not match the predicted charge distribution very well. Thus, while interpretation of the MFM response to stray fields above the iron film in terms of the micromagnetic model of Scheinfein *et al.* shows some agreement, there are troublesome length scale questions that must still be addressed.

The technique of magnetic force microscopy has been applied to domain wall structures in a 500-nm-thick ferromagnetic single crystal of iron. A wide variety of phenomena was observed in the sample, including Bloch walls, Bloch lines, and zig–zag walls. The structure of the Bloch walls has been discussed in terms of a two-dimensional micromagnetic model. Although the results presented are qualitative, several inconsistencies between modeled and measured data were determined. Work is in progress on more sophisticated, quantitative modeling of the MFM response to domain walls in iron, taking into account the extended nature of the tip, tip domain structure, and topographical effects between the tip and the sample surface.

This work was partially supported by the ONR, Grant No. N0014-89-J-1355. This is contribution 9309 of the Institute for Rock Magnetism. The Institute for Rock Magnetism is supported by grants from the Keck Foundation and the NSF.

[1] G. A. Prinz and J. J. Krebs, Appl. Phys, Lett. **39** (1981).
[2] U. Hartmann, J. Appl. Phys. **64**, 1561 (1988).
[3] H. J. Mamin, D. Rugar, J. E. Stern, R. E. Fontana, Jr., and P. Kasiraj, Appl. Phys. Lett. **55**, 318 (1989).
[4] S. Shtrikman and D. Treves, J. Appl. Phys. **31**, 147S (1960).
[5] A. Hubert, *Theorie der Domanenwande in Geordneten Medien* (Springer, Berlin, 1974), p. 246.
[6] M. R. Scheinfein, J. L. Blue, K. J. Coakley, D. T. Pierce, R. J. Celotta, and P. J. Ryan, Phys. Rev. B **43**, 3395 (1991); M. R. Scheinfein, R. J. Celotta, and D. T. Pierce, Phys. Rev. Lett. **63**, 668 (1989); M. R. Scheinfein, D. T. Pierce, and R. J. Celotta, J. Appl. Phys. **67**, 5932 (1990).
[7] B. A. Lilley, Philos. Mag. **41**, 792 (1950).
[8] U. Hartmann, Phys. Status Solidi A **101**, 227 (1987).